J_0 obtained from Fig. 3 can be used to calculate n_p and the result compared with a separate measurement of n_p using a calometric probe.[5] Taking measured values for δr, κ, and $(1-v_\perp^2/c^2)^{1/2}$, the calometric measurement and Fig. 3 yield $n_p = 2.4\times10^9$ cm^{-3} and $n_p = 2.9\times10^9$ cm^{-3}, respectively, giving agreement within an estimated experimental accuracy of $\pm 30\%$.

The authors wish to express their sincere thanks to Dr. T. K. Fowler and to the members of the Toroidal Confinement Group for their support in this work.

This work was performed under the auspices of the U. S. Atomic Energy Commission.

[1]N. C. Christofilos, in *Proceedings of the Second United Nations International Conference on the Peaceful Uses of Atomic Energy* (United Nations, Geneva, Switzerland, 1958), Vol. 32, p. 279.

[2]C. W. Hartman, Phys. Rev. Lett. 26, 826 (1971).

[3]S. Yoshikawa, Phys. Rev. Lett. 26, 295 (1971).

[4]O. A. Anderson, D. H. Birdsall, C. W. Hartman, E. B. Hooper, Jr., R. H. Munger, and C. E. Taylor, in *Proceedings of the Fourth International Conference on Plasma Physics and Controlled Nuclear Fusion Research, Madison, Wisconsin, 1971* (International Atomic Energy Agency, Vienna, 1971), Vol. 1, p. 103.

[5]O. A. Anderson, D. H. Birdsall, C. W. Hartman, E. B. Hooper, Jr., and R. H. Munger, Phys. Rev. Lett. 31, 10 (1973).

[6]O. A. Anderson, D. H. Birdsall, C. W. Hartman, E. B. Hooper, Jr., and R. H. Munger, Lawrence Livermore Laboratory Report No. UCRL-73984, 1972 (unpublished).

[7]C. W. Hartman and E. B. Hooper, Jr., to be published.

Velocity Autocorrelation Function and Dynamical Structure Factor of the Classical One-Component Plasma

J. P. Hansen* and E. L. Pollock†

Laboratoire de Physique Théorique et Hautes Energies, Université de Paris XI, 91405 Orsay, France‡

and

I. R. McDonald

Department of Chemistry, Royal Holloway College, Englefield Green, Surrey, England

(Received 5 December 1973)

We present molecular-dynamics computations of the velocity autocorrelation function and the dynamical structure factor of the classical one-component plasma. At high densities, the former exhibits marked oscillations, whereas the latter consists of very sharp peaks near the plasma frequency, up to wave vectors of order $1/a$, where a is the ion-sphere radius. The resulting dispersion curve is discussed.

We report here the results of a series of molecular-dynamics "experiments" on the *dynamical* properties of the fluid phase of the classical one-component plasma (OCP) in a uniform background of opposite charge. The work forms an extension of previously reported Monte Carlo computations of the *equilibrium* properties of the OCP.[1] Here we restrict ourselves to a discussion of the velocity autocorrelation function $Z(t)$ and dynamical structure factor $S(q,\omega)$; results on transverse currents and extensions to other systems of charged particles will be reported in a future publication.

Verlet's algorithm[2] was used to integrate numerically the classical equations of motion of a system of 250 ions, each with mass m and charge Ze. The usual periodic boundary conditions were imposed and the forces were calculated by an Ewald method[3] to account for the long range of the Coulomb interaction. As the unit of length we choose the ion-sphere radius $a = (3/4\pi\rho)^{1/3}$, where ρ is the number density, and as the unit of time we choose the inverse plasma frequency $\omega_p^{-1} = m/4\pi\rho(Ze)^2$. The configurational thermodynamic properties of the OCP are uniquely determined by the dimensionless parameter $\Gamma = (Ze)^2/akT$ and the Monte Carlo calculations have shown that the OCP crystallizes at $\Gamma = 155 \pm 10$.[1]

The present results are based on long molecular-dynamics runs (up to 10^5 time steps) at $\Gamma = 0.993$, $\Gamma = 9.7$, $\Gamma = 110.4$, and $\Gamma = 152.4$. The

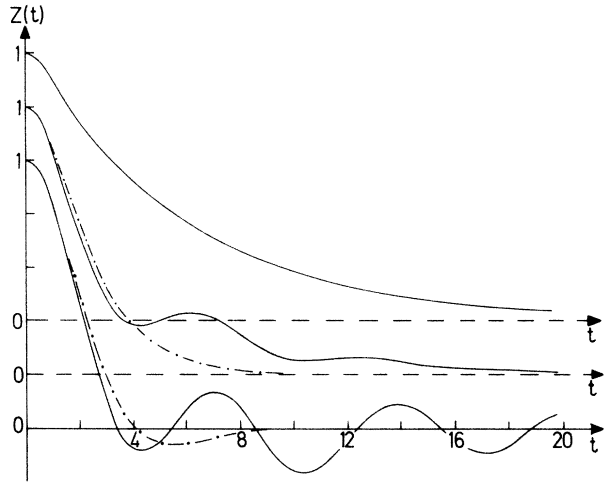

FIG. 1. Normalized velocity autocorrelation function for (reading from top to bottom) $\Gamma = 0.993$, 9.7 and 110.4. The dot-dashed lines give the result of the approximation (1). The time unit is $\sqrt{3}\ \omega_p^{-1}$.

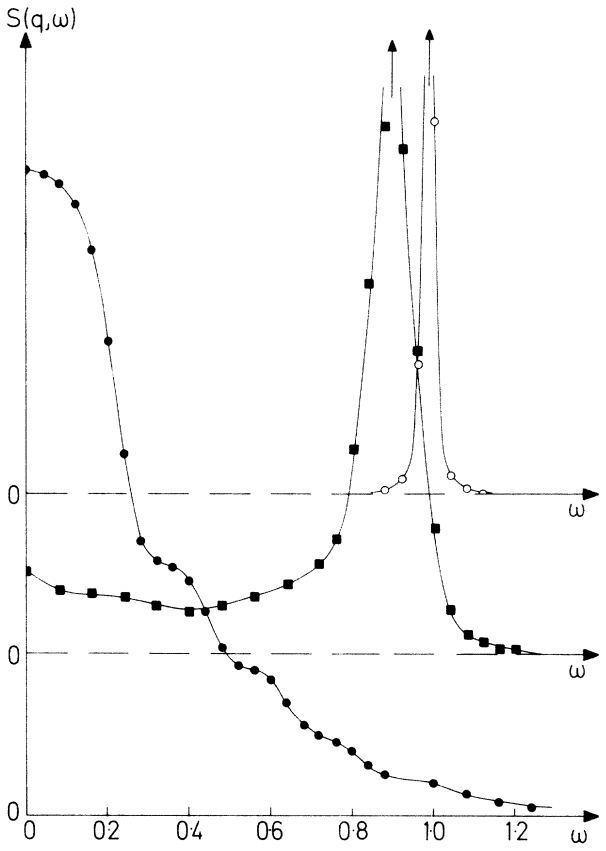

FIG. 2. Dynamical structure factor at $\Gamma = 110.4$ for $q = 0.619$ (open circles), 1.856 (squares), and 6.187 (filled circles) as a function of ω/ω_p. The vertical coordinate is arbitrary, but identical for the three q values.

collective dynamical properties of the OCP are expected to be strongly influenced by the plasma oscillations. Our computer "experiments" show that such effects are also important in the process of self-diffusion. In Fig. 1 we show the computed curves of $Z(t)$ for three values of Γ. The most striking feature at the higher Γ values is the appearance, at long times, of oscillations at a frequency near ω_p. The behavior of $Z(t)$ at short times can be analyzed by exploiting the fact that in the case of the Coulomb potential the second and fourth moments of $Z(t)$ have a particularly simple form. If we choose a Gaussian form to describe the generalized friction constant, or memory function $M(t)$, we may incorporate three moments exactly by writing

$$M(t) = \tfrac{1}{3} \exp(-2Jt^2), \tag{1}$$

where $J = \int_0^\infty r^{-4} g(r)\, dr$. Results obtained from the approximation (1) are also shown in Fig. 1 for the cases $\Gamma = 9.7$ and 110.4, so as to make it possible to distinguish the contributions to $Z(t)$ which arise from the pure diffusive mode and from the coupling of the latter to the collective modes of the system. We see that the behavior of $Z(t)$ at large times may be accounted for by including in $M(t)$ a long-time tail oscillating at a frequency close to ω_p. At $\Gamma = 9.7$ the tail in $M(t)$ represents an additional negative friction which enhances diffusion, but at $\Gamma = 110.4$ the net frictional effect is very much less, although the oscillations are more pronounced and decay more slowly. In fact, the approximation (1) leads to a diffusion coefficient D which differs by only 10% from the exact value. Finally, at $\Gamma = 0.993$ we find that Eq. (1) gives a very poor fit to $Z(t)$, even at short times; the predicted rate of decay is much too small. The reason is that the series expansion of $Z(t)$ diverges rapidly at low Γ; here $M(t)$ is virtually a δ function, so that $Z(t)$ is nearly exponential. The striking changes which occur in $Z(t)$ mean that D varies rapidly with Γ, decreasing by a factor of approximately 300 between $\Gamma = 0.993$ and $\Gamma = 110.4$.

We have investigated the longitudinal density fluctuations of the OCP by computing the dynamical structure factor $S(q, \omega)$ in the range $0 \leq \omega/\omega_p$

≤ 3, using the formula

$$S(q,\omega) = (1/2\pi N)\int_{-\infty}^{+\infty} e^{i\omega t}\langle \rho_{\vec{q}}(t)\rho_{-\vec{q}}(0)\rangle\, dt$$
$$= (1/2\pi N)\lim_{T\to\infty} T^{-1}\int_0^T e^{i\omega t}\rho_{\vec{q}}(t)\,dt\int_0^T e^{-i\omega t'}\rho_{-\vec{q}}(t')\,dt'$$
$$= (1/2\pi N)\lim_{T\to\infty} T^{-1}|\rho_{\vec{q}}(\omega)|^2,$$

where $\rho_{\vec{q}}(\omega)$ is the Fourier-Laplace transform of the density operator

$$\rho_{\vec{q}}(t) = \sum_{i=1}^{N}\exp[i\vec{q}\cdot\vec{r}_i(t)].$$

The most striking result of our computations is the appearance of very sharp peaks in $S(q,\omega)$ for wave vectors up to $q \simeq 2a^{-1}$ at $\Gamma = 110.4$ and 152.4. $S(q,\omega)$ is plotted for three q values, at $\Gamma = 110.4$, in Fig. 2. At the smallest q value compatible with the size of our system, the observed peak is extremely sharp and centered around a frequency close to ω_p; we are in the presence of a well-defined collective "plasmon" mode. At a q value which is roughly 3 times larger, the "plasmon" peak widens, but is still well defined; the position of the peak is shifted by about 10% towards the lower frequencies, and a "sidewing" develops at low frequencies. If the q value is increased by another factor of 3, the shape of $S(q,\omega)$ changes completely, and we obtain a Gaussian-like behavior, centered at the origin, which is already close to the free-particle result.

In Table I we list the positions and approximate widths of the lines observed at $\Gamma = 0.993$, 9.7, 110.4, and 152.4, for the five smallest q values investigated. From this table two important features emerge: (a) For a given q value, the collective modes are more strongly damped as Γ decreases, in qualitative agreement with the predictions of a simple random-phase–approximation claculation.[4] (b) If one plots the frequency $\omega(q)$ of the collective mode versus q, one observes that $\omega(q) \to \omega_p$ as $q \to 0$, as expected. At $\Gamma = 1$, $\omega(q)$ increase at small q, in agreement with the well-known result from Vlasov theory.[5] However, at the larger Γ values, $\omega(q)$ is a *decreasing* function of q. This qualitative change in the dispersion curve can be analyzed more closely by setting, for $\omega \geq 0$,

$$S(q,\omega) = A(q)\exp\{-[\omega-\omega(q)]^2/\sigma^2(q)\}. \tag{2}$$

$A(q)$, $\omega(q)$, and $\sigma(q)$ are determined by the exact moments of order 0, 2, and 4 of $S(q,\omega)$.[6] The following dispersion relation is obtained:

$$\omega^4(q) = \frac{\omega_p^4}{6}\left[\frac{q^4}{\Gamma^2 S^2(q)} - \frac{q^2}{S(q)}\left(\frac{q^2}{\Gamma^2}+\frac{1}{\Gamma}-\frac{2}{\Gamma}I(q)\right)\right], \tag{3}$$

where $S(q)$ is the structure factor, and

$$I(q) = \int_0^\infty \frac{dr}{r}[g(r)-1]\left(\frac{\sin qr}{qr}+\frac{3\cos qr}{q^2r^2}-\frac{3\sin qr}{q^3r^3}\right).$$

In the limit of small q, this yields, to order q^2,

$$\omega^4(q) = \omega_p^4[1 - q^2(\tfrac{5}{2}\delta + \tfrac{1}{2}\Gamma^{-1} + \tfrac{2}{45}\Gamma^{-1}U/NkT)], \tag{4}$$

where U/NkT is the configurational energy per particle, divided by kT, and δ is the coefficient of the q^4 term in the small-q expansion of $S(q)$:

$$S(q) \simeq (q^2/3\Gamma)(1+\delta q^2).$$

TABLE I. Frequency $\omega(q)$ and width $\sigma(q)$ (both in units of ω_p) of the $S(q,\omega)$ "plasmon" peaks, for five values of q (in units of a^{-1}) and four values of Γ.

Γ	0.993		9.7		110.4		152.4	
q	ω	σ	ω	σ	ω	σ	ω	σ
0.619	1.28	0.14	1.	0.05	0.99	~ 0.01	0.99	$\lesssim 0.01$
0.875	1.35	0.26	0.985	0.08	0.98	0.02	0.975	~ 0.01
1.383	1.42	···	0.97	0.12	0.94	0.03	0.935	0.02
1.856	···	···	0.94	0.24	0.90	0.05	0.89	0.03
2.315	···	···	0.86	···	0.80	0.24	0.80	0.15

The corresponding linewidth is given by

$$\sigma^2(q) = q^2(\tfrac{1}{2}\delta + \tfrac{1}{2}\Gamma^{-1} + \tfrac{2}{45}\Gamma^{-1}U/NkT)\omega_p{}^2.$$

Both U/NkT and δ are known from the computations of equilibrium properties.[1] U/NkT is always negative; δ is negative at $\Gamma = 1$, but becomes positive beyond $\Gamma \simeq 3$. Thus the coefficient of q^2 in (4) turns out to be positive for $\Gamma \lesssim 3$, and negative at higher Γ, in agreement with our observations. The high-Γ dispersion curve is not unlike the "optical" (longitudinal) phonon branch in the crystalline OCP.[1] This suggests that at high Γ "shearing" modes, related to the transverse motions, become important. This point is presently under investigation.

The authors are indebted to D. Levesque for supplying his efficient algorithm for computing $S(q,\omega)$, to B. Jancovici for stimulating discussions, and to Miss E. M. Gosling for programming the calculation of the Ewald sums. One of us (I.R.McD.) is grateful for the financial support of the United Kingdom Science Research Council.

*Present address: Laboratoire de Théorie des Liquides, Université de Paris VI, 4 Place Jussieu, Paris, France.

†Present address: Department of Physics, University of Illinois, Urbana, Ill. 61801.

‡Laboratoire associé au Centre National de la Recherche Scientifique.

[1]J. P. Hansen, Phys. Rev. A 8, 3096 (1973); E. L. Pollock and J. P. Hansen, Phys. Rev. A 8, 3110 (1973).

[2]L. Verlet, Phys. Rev. 159, 98 (1967).

[3]S. G. Brush, H. L. Sahlin, and E. Teller, J. Chem. Phys. 45, 2102 (1966).

[4]B. Jancovici, private communication; see also, e.g., D. Bohm and E. P. Gross, Phys. Rev. 75, 1851 (1949).

[5]N. G. Van Kampen and B. U. Felderhof, *Theoretical Methods in Plasma Physics* (North-Holland, Amsterdam, 1967), Chap. XI.

[6]P. G. de Gennes, Physica (Utrecht) 25, 825 (1959).

Direct Spectroscopic Observation of Electrons in Image-Potential States Outside Liquid Helium

C. C. Grimes and T. R. Brown
Bell Laboratories, Murray Hill, New Jersey 07974
(Received 26 November 1973)

We present the first direct spectroscopic study of electrons bound in image-potential–induced surface states outside liquid helium. We have observed absorption lines which show the expected linear Stark effect in the presence of an electric field. Zero-field splittings extrapolated from the data are 125.9 and 148.6 GHz for electronic transitions from the ground state to the first two excited states in the image-potential well.

The potential energy of an electron outside liquid helium is composed of two parts: (1) a long-range classical image potential, and (2) a short-range repulsive barrier at the surface. The latter is basically due to the exclusion principle, which forces the wave function of an extra electron to be orthogonal to those of the two electrons already present on each helium atom. The possibility that such a potential could cause surface states outside liquid helium was first noted by Sommer.[1] The idea was independently developed and further elaborated a few years later by Cole and Cohen,[2] and by Shikin.[3] Initial experimental investigations designed to measure the mobility[4] and lifetime[5] were apparently refuted by Ostermeier and Schwarz.[6] However, a cyclotron-resonance study by Brown and Grimes[7] showed the existence of surface states but gave no information about the potential. We are now presenting a direct spectroscopic study which shows conclusively the presence of an image-potential–induced surface state which displays a first-order linear Stark effect. In addition we are able to study the behavior of the image potential at the liquid-helium surface.

Our experiment consists of observing the absorption of microwave radiation by electrons on the surface of liquid helium. This is accomplished by tuning the splitting between the eigenstates in the image-potential well with an electric field until it is in resonance with our applied frequency. Observations are made at various applied frequencies and the unperturbed resonant frequencies are deduced by extrapolation to zero electric field.

We shall now briefly review the simple theory